THE JOURNAL OF BIOLOGICAL CHEMISTRY VOL. 288, NO. 1, pp. 608–618, January 4, 2013

Oncogenic MicroRNA-155 Down-regulates Tumor Suppressor *CDC73* and Promotes Oral Squamous Cell Carcinoma Cell Proliferation

IMPLICATIONS FOR CANCER THERAPEUTICS[*S]

Received for publication, October 5, 2012, and in revised form, November 17, 2012 Published, JBC Papers in Press, November 19, 2012, DOI 10.1074/jbc.M112.425736

Mohammad Iqbal Rather[‡], Mathighatta N. Nagashri[‡], Shivananda S. Swamy[§], Kodaganur S. Gopinath[§], and Arun Kumar[‡1]

From the [‡]Department of Molecular Reproduction, Development and Genetics, Indian Institute of Science, Bangalore 560012, India and the [§]Department of Surgical Oncology, Bangalore Institute of Oncology, 560027 Bangalore, India

Background: Cause of the complete loss of CDC73 in a subset of parathyroid tumors remains to be elucidated in the absence of a second mutation and promoter methylation.
Results: Oncogenic miR-155 causes down-regulation of tumor suppressor *CDC73* in OSCC.
Conclusion: miR-155 up-regulation adds yet another mechanism for CDC73 down-regulation in tumors.
Significance: Targeting miR-155 adds novelty to OSCC therapeutics.

The *CDC73* gene is mutationally inactivated in hereditary and sporadic parathyroid tumors. It negatively regulates β-catenin, cyclin D1, and c-MYC. Down-regulation of *CDC73* has been reported in breast, renal, and gastric carcinomas. However, the reports regarding the role of *CDC73* in oral squamous cell carcinoma (OSCC) are lacking. In this study we show that CDC73 is down-regulated in a majority of OSCC samples. We further show that oncogenic microRNA-155 (miR-155) negatively regulates *CDC73* expression. Our experiments show that the dramatic up-regulation of miR-155 is an exclusive mechanism for down-regulation of CDC73 in a panel of human cell lines and a subset of OSCC patient samples in the absence of loss of heterozygosity, mutations, and promoter methylation. Ectopic expression of miR-155 in HEK293 cells dramatically reduced CDC73 levels, enhanced cell viability, and decreased apoptosis. Conversely, the delivery of a miR-155 antagonist (antagomir-155) to KB cells overexpressing miR-155 resulted in increased CDC73 levels, decreased cell viability, increased apoptosis, and marked regression of xenografts in nude mice. Cotransfection of miR-155 with *CDC73* in HEK293 cells abrogated its pro-oncogenic effect. Reduced cell proliferation and increased apoptosis of KB cells were dependent on the presence or absence of the 3′-UTR in *CDC73*. In summary, knockdown of *CDC73* expression due to overexpression of miR-155 not only adds a novelty to the list of mechanisms responsible for its down-regulation in different tumors, but the restoration of *CDC73* levels by the use of antagomir-155 may also have an important role in therapeutic intervention of cancers, including OSCC.

The *CDC73* (cell division cycle 73, Paf1/RNA polymerase II complex component, homolog (*Saccharomyces cerevisiae*)), also known as *HRPT2* (hyperparathyroidism 2), is a tumor suppressor gene whose inactivation and mutation cause the hyperparathyroidism-jaw tumor syndrome. This syndrome is an autosomal dominant disorder characterized by the occurrence of parathyroid adenoma or carcinoma, fibro-osseous jaw tumors of the mandible or maxilla, and renal neoplastic and non-neoplastic abnormalities such as Wilm's tumor, hamartoma, and cystic renal disease (1–3). The 531-amino acid parafibromin encoded by *CDC73* forms polymerase-associated factor1 (Paf1) complex (4–6). As a part of Paf1, it remains associated with ribonucleic acid (RNA) polymerase II, regulates global gene expression, and is involved in coupling of transcriptional and posttranscriptional events (7–10).

CDC73 overexpression is documented to inhibit colony formation and cellular proliferation and induces cell cycle arrest in the G_1 phase, indicating that it has a critical role in cell growth and proliferation (11). Furthermore, BTK (Bruton's tyrosine kinase) has been found to increase the abundance of CDC73 in the absence of WNT3A stimulation, and in turn CDC73 acts as a repressor of β-catenin-mediated transcription in human colorectal cancer cells and B cells (12). These findings suggest the potential role of CDC73 in pathogenesis and progression of malignancies.

Besides mutations (predominantly), the loss of heterozygosity and promoter methylation of *CDC73* in tumors has been reported as having different mechanisms for its down-regulation (13, 14). But there are also reports where methylation was not identified in any specimens despite a complete loss of parafibromin expression in parathyroid carcinomas with a single detectable *CDC73* mutation and retention of the wild-type *CDC73* allele (15). Furthermore, no mutations of possibly pathogenic nature were identified in the 5′-UTR of *CDC73* (15). These data strongly suggest that some other mechanisms such as mutations in *CDC73* intronic regions, alternate epigenetic regulation (*e.g.* histone modifications), or other regulatory inactivation mechanisms (*e.g.* targeting by microRNAs) may play a role in the loss of *CDC73* expression. Regulation of CDC73 expression has been studied at transcriptional and posttran-

* This work was supported by the University Grants Commission (New Delhi).
[S] This article contains supplemental Table S1.
[1] To whom correspondence should be addressed. Tel.: 91-80-2293-2998; Fax: 91-80-2360 0999; E-mail: karun@mrdg.iisc.ernet.in.

scriptional levels. Although BTK has been found to increase CDC73 level, it has been shown by quantitative polymerase chain reaction analysis of patient-derived B cells that *CDC73* transcripts were unexpectedly more abundant in cells lacking BTK, but its protein level was low (12). This suggests that the availability of its protein level is determined by some posttranscriptional mechanisms (12). Therefore, a clear understanding of the post-transcriptional regulation of *CDC73* will be of tremendous scientific and clinical significance.

Squamous cell carcinoma accounts for more than 95% of the carcinomas of the oral cavity (16). Oral squamous cell carcinoma (OSCC)[2] in developing countries is the sixth most common cancer in males and tenth in females (16). In India it is the leading cancer in males and third most common malignancy in females (17). The five-year survival rate of OSCC lacks any improvements, and the efforts to develop an appropriate therapeutic strategy still lies in catch 22, demanding the identification of molecular markers and signaling pathways for better prognosis and therapeutic intervention of OSCC (17).

Being a multigenic disease, the single gene-based therapy of OSCC may fall short in therapy (18). Recent studies have shown that a growing class of noncoding RNAs called microRNAs (miRNAs) are involved in posttranscriptional regulation of genes (19). There is a growing body of literature supporting the potential role of miRNAs in regulation of cancer (20). The importance of *CDC73* in the orchestration of several cellular functions and the prediction for its posttranscriptional regulation makes it an attractive candidate for miRNA-mediated regulation of cell growth and proliferation.

Here we report the identification of an oncogenic microRNA-155 (miR-155) that regulates the expression of tumor suppressor gene *CDC73*. Furthermore, restoration of *CDC73* levels by the use of antagomir-155 warrants a prolific strategy to treat cancers, including OSCC.

MATERIALS AND METHODS

Sample Collection—A total of 22 matched OSCC samples and normal oral tissues from the patients were ascertained at the Bangalore Institute of Oncology, Bangalore, India. All tumor samples were mostly from the tongue and cheek areas of the mouth. This study was performed with informed consent from the patients and approval from the ethics committee of the Bangalore Institute of Oncology. The clinicopathological data for 22 patients are given in supplemental Table S1. Tumors were classified according to tumor, node, and metastasis criteria (21).

In Silico Identification of miRNA Binding Sites—We used a consensus approach by employing a total of six established target prediction programs (Table 1) to perform target prediction (22). We selected only miRNA, which is detected by all the six programs, to bind to the same site in the target 3′-UTR. Because inaccessibility to the region of binding may be due to strong local secondary structure, we therefore carried out the ΔG analysis for 70 bases on each side flanking to the miRNA binding site using the mFold software (23).

Plasmid Constructs—To generate the pcDNA3.1(+)-bic construct expressing the miR-155, *BIC* (B-cell integration center) exon 3 sequence was amplified using primers as described by Eis *et al.* (24) with certain modification that included incorporation of different restriction enzyme sites in the primers to facilitate directional cloning and human genomic DNA as a template. Similarly, the pcDNA3.1(+)-dme-mir-4 construct harboring the *Drosophila melanogaster* mir-4 was generated using *D. melanogaster* genomic DNA as a template in amplification reactions. To generate constructs with *CDC73* 3′-UTR at the 3′ end of the luciferase ORF in the pMIR-REPORT vector (Invitrogen), a 1214-base pair-long *CDC73* 3′-UTR from position +1595 to +2809 was amplified from human genomic DNA and cloned both in sense and antisense manner using a standard laboratory method. The sense, mutant, and antisense constructs were designated as pMIR-REPORT-3′-UTR-sense, pMIR-REPORT-3′-UTR-mutant, and pMIR-REPORT-3′-UTR-antisense, respectively. The mutant 3′-UTR was generated by site-directed mutagenesis by deleting bases 2–7 from the seed region of miR-155 binding site using pMIR-REPORT-3′-UTR-sense as a template. The pcDNA3-HA-Pf (pcDNA3-HA-CDC73) construct harboring a full-length *CDC73* ORF was a kind gift from Dr. F. Kowalke from ETH, Zurich. The pcDNA3-HA-CDC73–3′-UTR-sense construct harboring the intact 3′-UTR was generated by amplifying and cloning of the 3′-UTR sequence downstream of the *CDC73* ORF at XhoI and ApaI sites in pcDNA3-HA-CDC73. The pcDNA3-HA-CDC73-3′-UTR-mutant construct was generated by site-directed mutagenesis using pcDNA-HA-CDC73–3′-UTR-sense as a template and specific primers. All the constructs were sequenced on an ABIprism A310-automated sequencer (Invitrogen) to ascertain directionality and error free sequence of the inserts. Details of the primers used for cloning are available on request from the authors.

Cell Culture, Transient Transfection, and Reporter Assays—Human cell lines HEK293 (embryonic kidney), HEK293T (embryonic transformed kidney), A549 (lung adenocarcinoma), HeLa (cervical carcinoma), KB (oral squamous cell carcinoma), SCC084 (oral squamous cell carcinoma), and SCC131 (oral squamous cell carcinoma) were maintained in DMEM supplemented with 10% fetal bovine serum and 1x antibiotic/antimycotic solution (Sigma) in a humidified chamber with 5% CO_2 at 37 °C. HEK293, HEK293T, A549, HeLa, and KB cells were procured from the National Centre for Cell Science, Pune, India. SCC084 and SCC131 cells were kind gifts from Prof. Susanne Gollin, University of Pittsburgh, Pittsburgh, PA.

For overexpression studies, 2×10^6 cells/well in a 6-well plate were transfected with an appropriate construct or a combination of constructs using Lipofectamine™ 2000 (Invitrogen) according to the manufacturer's instructions. Luciferase reporter gene assays were performed post 24 or 48 h of transfection using the Dual-Luciferase® Reporter Assay System (Promega, Madison, WI) according to the manufacturer's protocol. Cells were also co-transfected with the pRL-TK control vector (Promega), encoding Renilla luciferase for normalizing transfection efficiency. Different stable transfectants in KB cells were generated by the pooling of clones acquired after KB cells

[2] The abbreviations used are: OSCC, oral squamous cell carcinoma; miRNA, microRNA; miR-155, microRNA-155; CASP3, caspase-3; MTT, 3-(4,5-dimethylthiazol-2-yl)-2,5-diphenyltetrazolium bromide; Alu, Alu sequence.

were continuously grown in G418 containing selection medium post 48 h of transfection.

Total RNA Extraction and RT-PCR—Total RNA was isolated from different cell lines using the TRI-Reagent™ (Sigma) according to the manufacturer's instructions. RNA was stored at −70 °C until further use. cDNA was made using a first-strand cDNA synthesis kit (Fermentas, Ontario, Canada). RT-PCR was performed using primers specific to *CDC73* and *GAPDH* following a standard protocol. Details of the primers used for RT-PCR are available on request from the authors.

miR-155 Northern Hybridization—Total RNA (50 μg) samples were run on a 15% acrylamide gel under denaturing conditions, transferred onto a N^+Biodyne nylon membrane (Pall, Port Washington, NY), and hybridized with a γ-^{32}P-labeled probe (5′-ACCCCTATCACGATTAGCATTAA-3′) specific to the antisense strand of human miR-155. Hybridization was performed overnight at 42 °C in a hybridization buffer containing 5× SSC, 20 mM NaH_2PO_4, pH 7.5, 7% SDS, 2× Denhardt's solution, and 40 ng/ml sheared salmon sperm DNA. Subsequently, the membrane was washed in 3× SSC, 25 mM NaH_2PO_4, pH 7.5, 5% SDS, and 10× Denhardt's solution twice for 5 min each followed by washing in 1× SSC and 1% SDS once for 5 min. The membrane was dried and exposed to a phosphorimaging screen (Fujifilm, Japan) for 48 h. As a loading control, a γ-^{32}P-labeled probe (5′-GCTAATCTTCTCTGTATCGTTCCA) specific to the U6 RNA was used.

Western Hybridization—Whole protein lysates were prepared using the CelLytic™ M Cell Lysis Reagent (Sigma). They were resolved on a SDS-PAGE and transferred to a BioTrace PVDF nylon membrane (Pall, Port Washington, NY) using a semi-dry transfer apparatus. The membrane was blocked using 5% fat-free milk powder in 1× PBS-Tween, and the signal was visualized using a 1:750 dilution of an anti-CDC73 antibody either from Santa Cruz Biotechnology (catalog #2H1) or from Sigma (product #C3620). After incubation with a horseradish peroxidase linked secondary antibody, the signal was detected using the Immobilon™ Western Chemiluminescent HRP substrate (Millipore, Billerica, MA) and x-ray films. The mouse β-actin and HA epitope antibodies were purchased from Sigma.

miR-Q RT-PCR—The miR-155 expression analysis was carried out by miR-Q, a method developed by Sharbati-Tehrani *et al.* (25) for the expression analysis of miRNA by RT-PCR. The expression of miR-155 in OSCC samples was compared with normal tissues using the $2^{-\Delta\Delta CT}$ method and 5 S rRNA as a normalizing control (26).

Mutation Analysis—The entire coding region of *CDC73* including its exon/intron junctions was amplified using gene-specific primers and sequenced on an ABIprism A310-automated sequencer. Details of the primers used for mutation analysis are available on request from the authors.

LOH Analysis at the CDC73 Locus—For LOH studies, total genomic DNA from blood, and tissue samples was isolated using the Wizard® Genomic DNA purification kit (Promega) according to the manufacturers' instructions. Matched normal and tumor DNA samples were genotyped using four highly polymorphic microsatellite markers: three extragenic markers (D1S384, D1S422, and D1S408) and one intragenic marker (para14M) present in intron 14 of *CDC73*. Details of the first three markers were retrieved from the UCSC Genome Bioinformatics site. Details of the internal marker were adapted from a previous report (1).

Combined Bisulfite Restriction Analysis—Methylation status of the *CDC73* promoter described by Hewitt *et al.* (14) was examined by combined bisulfite restriction analysis (COBRA) using AciI and BstUI enzymes following a standard procedure in our laboratory (27).

Cell Proliferation Assay—The cell proliferation was measured by the MTT assay as described previously (28). In brief, 48 h of post transfection of HEK293 or KB cells in 6-well plates with different constructs, antagomir-155 (catalog #AM17000; Invitrogen) or scrambled oligo (catalog #AM17010, Invitrogen), transfection medium in each well was replaced by 100 μl of fresh serum-free medium with 0.5 g/liter MTT. After incubation at 37 °C for 4 h, the MTT medium was aspirated out, and 50 μl of DMSO was added to each well. After incubation at 37 °C for another 10 min, the absorbance value of each well was measured using an ELISA plate reader (Bio-Rad) at 595 nm. The relative cell proliferation rate was calculated according to Jiang *et al.* (28).

Apoptosis Assay—The rate of apoptosis was measured using the CaspGLOW™ Fluorescein Active Caspase-3 Staining kit (BioVision, Milpitas, CA) using the manufacturer's protocol. The kit provides a sensitive detection of activated caspase-3 (CASP3) in living cells. It utilizes the CASP3 inhibitor, DEVD-fluoromethyl ketone, conjugated to FITC (FITC-DEVD-FMK) as a marker. Briefly, 1×10^6 cells were grown in 6-well plates to about 60% confluence and transiently transfected with pcDNA3.1(+)-dme-mir-4, pcDNA3.1(+)-bic, antagomir-155, or scrambled oligo. Post 48 h of transfection, cells were resuspended in a complete DMEM and incubated with FITC-DEVD-fluoromethyl ketone conjugate for 1.5 h in dark. Post incubation, cells were washed and finally suspended in 300 μl of wash buffer. Cells were then analyzed with the FACSCalibur flow cytometer (BD Biosciences). The relative cell apoptosis rate was calculated according to Jiang *et al.* (28). The same protocol was used to assess the rate of apoptosis of different stable KB transfectants.

Soft Agar Assay—Tumor cells have the propensity to grow in an anchorage-independent manner and hence can form colonies in a semi-solid medium such as soft agar. The anchorage-independent growth of the stable *CDC73* and vector clones was analyzed by the soft agar assay in 35-mm tissue culture dishes by following a standardized protocol.

Propidium Iodide Analysis—The proliferation of stable vector and *CDC73* clones was analyzed by the FACSCalibur flow cytometer after staining the cells with propidium iodide (Sigma) following a standard protocol.

In Vivo Assay for Tumor Growth—To see the effect of restoration of CDC73 expression by inhibition of miR-155 on tumor growth, 2×10^6 KB cells were transfected separately with 200 nM antagomir-155 or mock (scrambled oligos). Post 24 h of transfection, 3×10^6 cells were suspended in 150 μl of Dulbecco's modified phosphate buffer and then subcutaneously injected into the right posterior flank of each female BALB/c athymic 6-week-old nude mouse. Tumors of measurable size

TABLE 1
A list of predicted miRNAs having potential binding sites in the 3-UTR of *CDC73* and binding free energy around the potential binding site of hsa-miR-155
hsa, *Homo sapiens*.

Algorithms for the prediction of miRNA targeting *CDC73*					
DIANA-microT	**PicTar**	**Miranda**	**TargetScan**	**MirTarget2**	**Microcosm**
hsa-miR-9	hsa-miR-211	hsa-miR-128a	hsa-miR-216/216b	hsa-miR-579	hsa-miR-155
hsa-miR-429	hsa-miR-204	hsa-miR-188-5p	hsa-miR-181	hsa-miR-664	hsa-miR-188-5p
hsa-miR-200c	hsa-miR-181c	hsa-miR-155	hsa-miR-24	hsa-miR-885-5p	hsa-miR-487a
hsa-miR-200b	hsa-miR-181a	hsa-miR-20b*	hsa-miR-181	hsa-miR-28-5p	hsa-miR-708
hsa-miR-300	hsa-miR-181b	hsa-miR-26b*	hsa-miR-199/199-5p	hsa-miR-1248	
hsa-miR-381	hsa-miR-199a	hsa-miR-28-5p	hsa-miR-9	hsa-miR-708	
hsa-miR-181d	hsa-miR-9	hsa-miR-323-3p	hsa-miR-155	hsa-miR-199a-5p	
hsa-miR-181d	hsa-miR-199b	hsa-miR-34b	hsa-miR-490/490-3p	hsa-miR-155	
hsa-miR-579	hsa-miR-155	hsa-miR-362-5p	hsa-miR-150	hsa-miR-199b-5p	
hsa-miR-885-5p		hsa-miR-367	hsa-miR-216/216a	hsa-miR-186	
hsa-miR-155		hsa-miR-487a	hsa-miR-217	hsa-miR-380	
		hsa-miR-499-3p	hsa-miR-181	hsa-miR-516a-3p	
		hsa-miR-566	hsa-miR-7/7ab	hsa-miR-2052	
		hsa-miR-656	hsa-miR-204/211	hsa-miR-381	
		hsa-miR-708	hsa-miR-383	hsa-miR-300	
		hsa-miR-801		hsa-miR-149	
				hsa-miR-337-3p	

Type of miRNA	ΔG for 5'70bp(kcal/mol)	ΔG for 3'70bp(kcal/mol)
hsa-miR-155	-2.87	-2.66

appeared post 1 week of injection. Tumor growth was monitored, and its volume was measured using a digital caliper for every 3 days till 23 days. Tumor volume (V) was calculated as $V = L \times W^2 \times 0.5$, where L and W represent length and width, respectively. Tumor weight was taken at the end of the study. All nude mice experiments were approved by the institutional animal ethics committee.

Statistical Analysis—An independent two-tailed Student's t test was performed to determine the significance of difference between two experiments.

RESULTS

Identification of miR-155 as a Regulator of CDC73—To predict the miRNAs that may regulate *CDC73*, we used a consensus approach by employing six different miRNA target prediction algorithms such as DIANA-microT, PicTar, Miranda, TargetScan, MirTarget2, and Microcosm. We found that several miRNAs have potential binding sites in the 3′-UTR of *CDC73* (Table 1). These miRNA binding sites are evenly scattered all over the 3′-UTR. We preferentially picked up miR-155 for its validation because all target prediction algorithms predicted it targeting the *CDC73* (Table 1). Our bioinformatics analysis predicted the binding of miR-155 to the 3′-UTR of *CDC73* in a region encompassing +1831 to +1854 bases (Fig. 1*A*). The Δ*G* analysis showed that the miR-155 binding region in the 3′-UTR has a very weak secondary structure (Table 1). The ClustalW alignment of miRNA seed region binding site in the 3′-UTR of *CDC73* showed that it is conserved in different species (Fig. 1*A*), underscoring that miR-155 may have a basal role to play in regulating *CDC73* expression.

Effect of miR-155 Overexpression on CDC73 Expression—To validate if miR-155 regulates *CDC73* expression, a panel of human cell lines (*viz.*, A549, HeLa, KB, SCC084, and SCC131) was examined for miR-155 expression by Northern blot analysis. The expression of miR-155 was easily detectable in KB cells, whereas it was not detectable in other cell lines even after loading 50 μg of total RNA (Fig. 1*B*, *upper panel*). To see whether this differential expression of miR-155 in KB cells is reflected with a low expression of its predicted target *CDC73*, total protein lysates were prepared from these cell lines and examined for *CDC73* expression by Western blotting. CDC73 was barely detectable in KB cells as compared with other cell lines (Fig. 1*B*). Also, KB cells did not show any *CDC73* promoter methylation and mutation upon analysis, suggesting the regulation of *CDC73* by miR-155.

The pcDNA3.1(+)-bic construct coding for miR-155 was transiently transfected into HEK293T cells followed by Northern and Western blot analyses to check for the expression of miR-155 and CDC73, respectively. The results showed that, as expected, miR-155 down-regulated CDC73 in a dose-dependent manner, whereas the control pcDNA3.1(+)-dme-mir-4 construct coding for an irrelevant *D. melanogaster* mir-4 had no effect (Fig. 1*C*). It is interesting to note that the level of *CDC73* transcript remained constant (Fig. 1*C*). Thus, it is most likely that miR-155 decreases *CDC73* expression by inhibiting its translation.

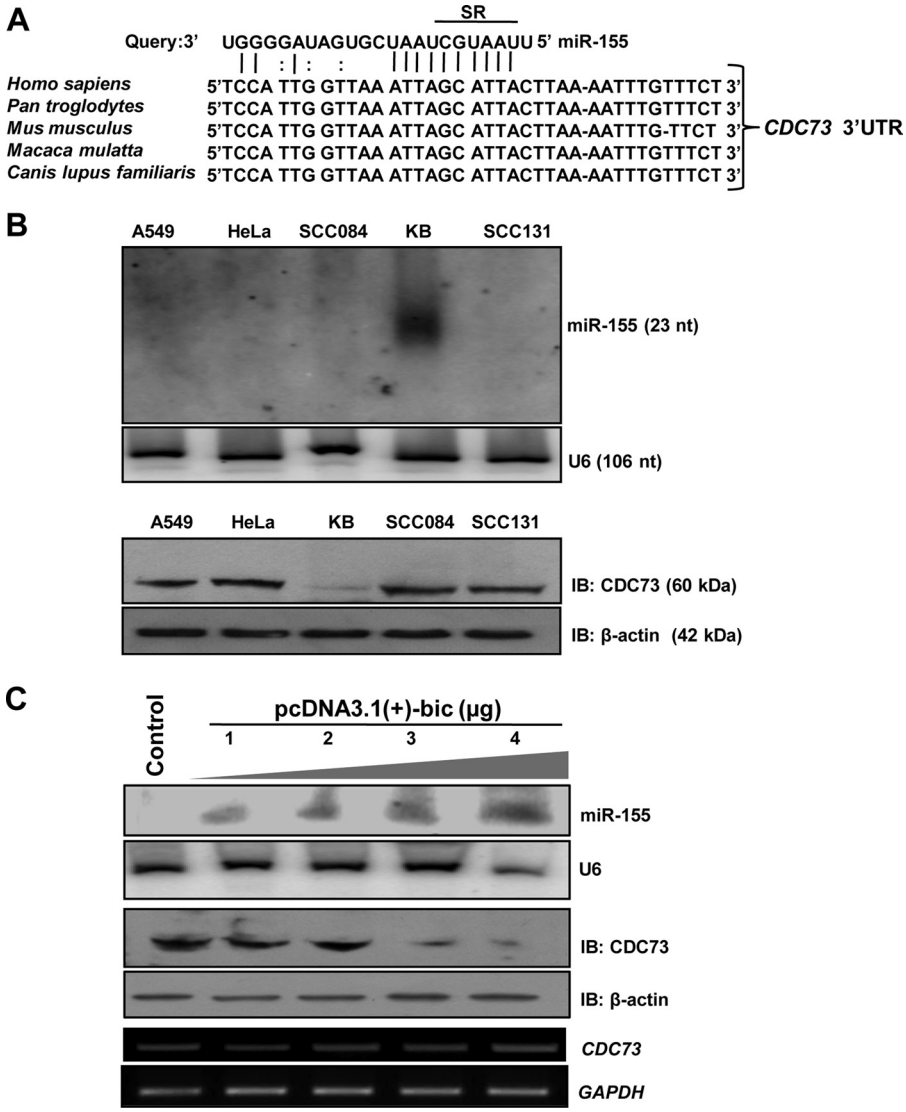

FIGURE 1. **Identification of miR-155 as a regulator of *CDC73* expression.** *A*, shown is a putative miR-155 binding site within the *CDC73* 3′-UTR (GenBank™ accession no. NM_024529.0). Perfect matches and G:U (or G:T) pairs are indicated by *vertical lines* and *colons*, respectively. The ClustalW alignment shows that the putative miR-155 binding site is conserved in different species. *SR* (seed region) denotes the seed region. *B*, shown is expression analysis of miR-155 and CDC73 in A549, HeLa, SCC084, KB, and SCC131 cells. Note the expression of miR-155 only in KB cells (*upper panel*). Also note the reduced expression of CDC73 in KB cells as compared with other cell lines (*lower panel*), suggesting that miR-155 negatively regulates CDC73. The expression of miR-155 and CDC73 was analyzed by Northern and Western hybridizations, respectively. *C*, shown is the effect of miR-155 overexpression on CDC73 expression in HEK293T cells. For overexpression of miR-155, 1–4 μg of pcDNA3.1(+)-bic was transfected in HEK293T cells. The *Control lane* represents transfection of HEK293T cells with the *D. melanogaster* miRNA dme-mir-4-expressing construct pcDNA3.1(+)-dme-mir-4 that does not have any mammalian target as shown by prediction programs used in this study. Note the overexpression of miR-155 led to reduced CDC73 expression in a dose-dependent manner. *U6 RNA*, *GAPDH*, and β-actin were used as loading controls for Northern, RT-PCR, and Western hybridization, respectively. *IB*, immunoblot; *nt*, nucleotides.

Confirmation of Target Site for miR-155 in CDC73 3′-UTR—When HEK293T cells were cotransfected with pcDNA3.1(+)-bic coding for miR-155 and pMIR-REPORT-3′-UTR-sense containing the intact *CDC73* 3′-UTR in a sense orientation, we observed a significantly reduced luciferase reporter expression compared with cells transfected with pMIR-REPORT-3′-UTR-sense (Fig. 2*A*). However, when HEK293T cells were cotransfected with pMIR-REPORT-3′-UTR-sense and pcDNA3.1(+)-dme-mir-4 constructs, there was no significant effect on luciferase expression compared with cells transfected with pMIR-REPORT-3′-UTR-sense (Fig. 2*A*). Most importantly, when pcDNA3.1(+)-bic was cotransfected with pMIR-REPORT-3′-UTR-mutant containing the mutated binding site or pMIR-REPORT-3′-UTR-antisense containing the intact *CDC73* 3′-UTR in an antisense orientation and lacking the miR-155 binding site in HEK293T cells, there was no significant reduction in the luciferase expression as compared with cells transfected with pMIR-REPORT-3′-UTR-sense (Fig. 2*A*). Also, when the pMIR-REPORT-3′-UTR-sense construct was transfected in KB cells with a high level of endogenous miR-155, the luciferase expression was significantly reduced as compared with KB cells with the control pMIR-REPORT vector (Fig. 2*B*). This down-regulation was not seen in KB cells transfected with either pMIR-REPORT-3′-UTR-antisense or pMIR-REPORT-3′-UTR-mutant (Fig. 2*B*). No change in the luciferase expression was observed in SCC131 cells with an undetectable expression of miR-155 after transfection of any of these constructs in comparison to SCC131 cells transfected with pMIR-REPORT

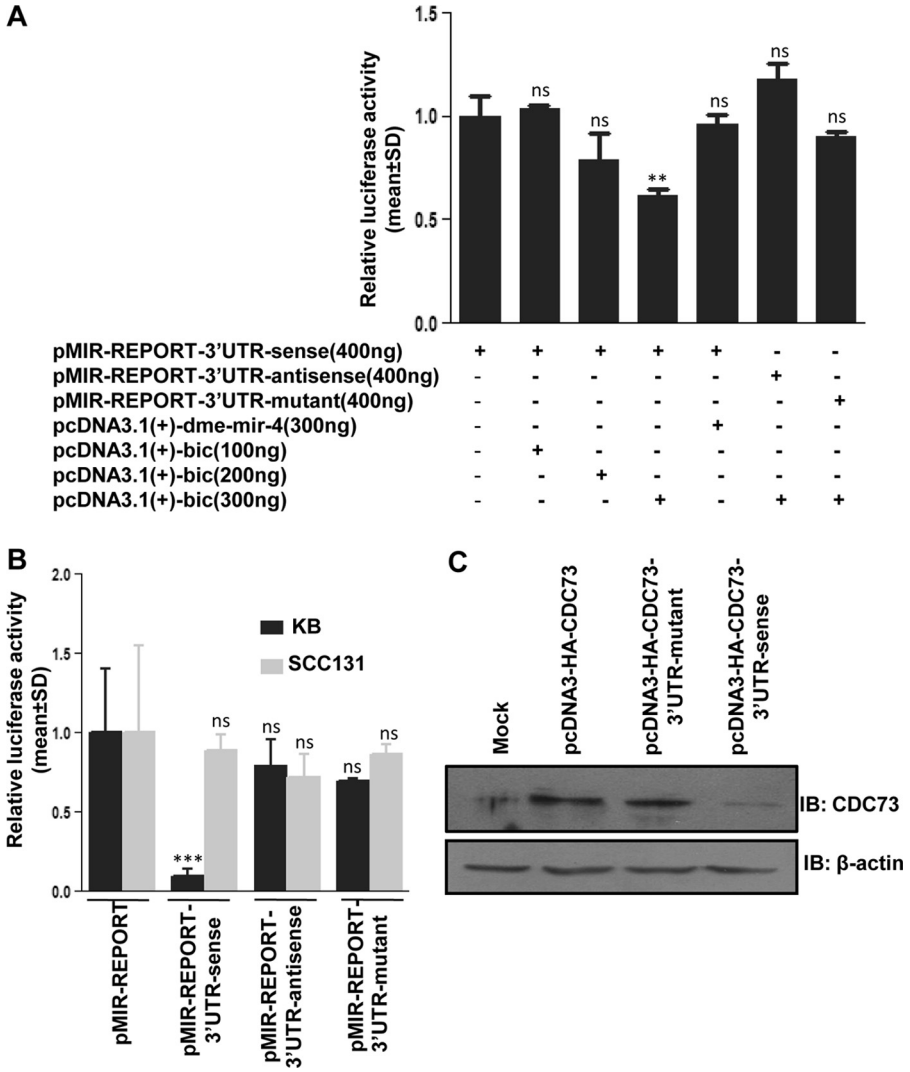

FIGURE 2. **Confirmation of the miR-155 target site in the *CDC73* 3′-UTR.** *A*, miR-155 reduces luciferase expression in HEK293T cells by binding to a target site in the *CDC73* 3′-UTR. Note that an increasing concentration of pcDNA3.1(+)-bic significantly reduces the luciferase expression in cells co-transfected with pMIR-REPORT-3′-UTR-sense construct compared with cells transfected with pMIR-REPORT-3′-UTR-sense alone, whereas the luciferase expression does not change in cells co-transfected with pcDNA3.1(+)-bic and pMIR-REPORT-3′-UTR-antisense or pMIR-REPORT-3′-UTR-mutant constructs compared with cells transfected with p-MIR-REPORT-3′-UTR-sense construct alone. Also note that the luciferase expression does not change in cells co-transfected with pMIR-REPORT-3′-UTR-sense and pcDNA3.1(+)-dme-mir-4 constructs compared with cells transfected with p-MIR-REPORT-3′-UTR-sense construct alone, suggesting that miR-155 reduces the luciferase expression by binding to a specific site in the *CDC73* 3′-UTR. The total DNA for each transfection was adjusted to 800 ng with the pcDNA3.1(+) vector. *B*, the effect of endogenous miR-155 on luciferase reporter expression is shown. The luciferase reporter vector pMIR-REPORT (control) and luciferase reporter constructs with *CDC73* 3′-UTR, pMIR-REPORT-3′-UTR-sense, pMIR-REPORT-3′-UTR-mutant, and pMIR-REPORT-3′-UTR-antisense were transfected individually in KB and SCC131 cells, and the luciferase expression was measured post-24 h of transfection. Note a reduced expression of luciferase reporter in KB cells with pMIR-REPORT-3′-UTR-sense construct as compared with cells transfected with the pMIR-REPORT vector, pMIR-REPORT-3′-UTR-mutant, or pMIR-REPORT-3′-UTR-antisense constructs. This is due to the fact that a high endogenous level of miR-155 is able to bind the *CDC73* 3′-UTR in a sense orientation and inhibit translation of the luciferase reporter. Also note that the luciferase expression does not change in SCC131 cells with an undetectable level of miR-155 when these cells were transfected with the pMIR-REPORT vector, pMIR-REPORT-3′-UTR-sense, pMIR-REPORT-3′-UTR-mutant, or pMIR-REPORT-3′-UTR-antisense constructs. *C*, shown is the effect of an endogenous level of miR-155 on the expression of *CDC73* with or without its 3′-UTR in KB cells. Note a reduced expression of CDC73 in cells transfected with the construct pcDNA3-HA-CDC73–3′-UTR-sense having its 3′-UTR in a sense orientation as compared with cells transfected with the construct pcDNA3-HA-CDC73 without its 3′-UTR or the construct pcDNA3-HA-CDC73–3′-UTR-mutant with its mutated miR-155 binding site, underscoring that miR-155 targets *CDC73* by binding to its 3′-UTR. *Mock* represents cells transfected with the pcDNA3-HA vector. $n = 3$; *ns*, data are statistically non-significant; **, $p < 0.01$; ***, $p < 0.001$. *IB*, immunoblot.

(Fig. 2*B*). Furthermore, as expected, when KB cells having a high endogenous level of miR-155 were stably transfected with the *CDC73* construct pcDNA3-HA-CDC73–3′-UTR-sense, the expression of CDC73 was reduced compared with cells transfected with either pCDNA3-HA-CDC73 lacking the 3′-UTR or pcDNA3-HA-CDC73–3′-UTR-mutant (Fig. 2*C*). These experiments clearly indicated that the mature miR-155 regulates *CDC73* expression by interacting with its 3′-UTR in a site-specific manner.

CDC73 Overexpression Is Dependent on the Presence or Absence of Its 3′-UTR—To assess the role of *CDC73* 3′-UTR in the regulation of its expression and hence its function, *CDC73* constructs with and without 3′-UTR were stably transfected into KB cells. We chose this cell line because it has a high expression of miR-155 and a low level of CDC73 (Fig. 1*B*). We then assessed the rate of proliferation and apoptosis of KB cells stably transfected with different *CDC73* constructs by FACS analysis of propidium iodide-stained cells, MTT, soft agar, and

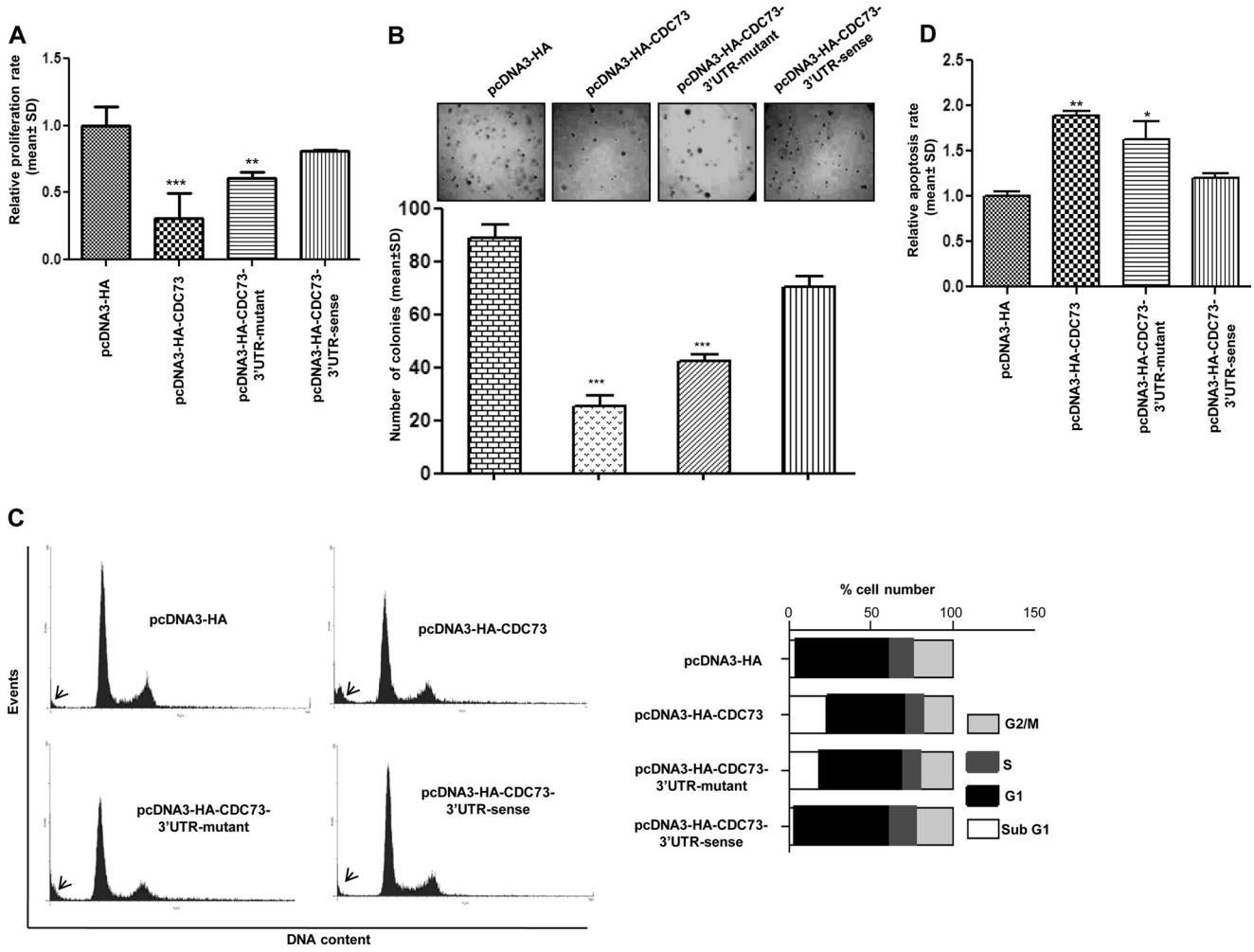

FIGURE 3. **Anti-tumorigenic function of *CDC73* in KB cells.** *A*, shown is a quantitative analysis of cell proliferation by the MTT assay. Note a significantly reduced proliferation of KB cells transfected with either pcDNA3-HA-CDC73 or pcDNA3-HA-CDC73–3′-UTR-mutant constructs compared with cells transfected with either pcDNA3-HA (vector control) or pcDNA3-HA-CDC73–3′-UTR-sense construct. *B*, shown is an assessment of tumorigenic potential of KB cells by the soft agar assay. Note a reduction in the number of colony formation by KB cells transfected with either pcDNA3-HA-CDC73 or pcDNA3-HA-CDC73–3′-UTR-mutant constructs compared with cells transfected with either pcDNA3-HA or pcDNA3-HA-3′-UTR-CDC73-sense construct. The *lower panel* is a graphical representation of the soft agar data. *C*, shown is a FACS analysis of propidium iodide-stained KB cells stably transfected with the pcDNA3-HA vector and different CDC73 constructs. The sub-G_1 population (cells undergoing death) is marked by *arrows*. Note an increase in sub-G_1 population of cells transfected with either pcDNA3-HA-CDC73 or pcDNA3-HA-CDC73–3′-UTR-mutant constructs compared with cells transfected with either pcDNA3-HA or pcDNA3-HA-CDC73–3′-UTR-sense. A graphical representation of the data is shown on the *right*. *D*, shown is the assessment of the rate of apoptosis by the CASP3 assay. Note a significantly increased rate of apoptosis in KB cells transfected with either pcDNA3-HA-CDC73 or pcDNA3-HA-CDC73–3′-UTR-mutant constructs compared with cells transfected with either pcDNA3-HA or pcDNA3-HA-CDC73–3′-UTR-sense. $n = 3$; *, $p < 0.05$; **, $p < 0.01$; ***, $p < 0.001$.

CASP3 assays. Compared with KB cells harboring the pcDNA3-HA vector or the pcDNA3-HA-CDC73–3′-UTR-sense construct with an intact 3′-UTR, proliferation and anchorage-independent growth of cells stably transfected with pcDNA3-HA-CDC73 (lacking 3′-UTR) and pcDNA3-HA-CDC73–3′-UTR-mutant were significantly decreased (Fig. 3, *A* and *B*), whereas the rate of apoptosis was significantly increased (Fig. 3, *C* and *D*). These experiments not only underscore the fact that *CDC73* has a definite role in regulating cell growth and proliferation but also give an insight that miR-155 is exercising its oncogenic role by targeting *CDC73*.

Regulation of Cell Growth and Proliferation by CDC73 as a Target of miR-155—To confirm further that the miR-155-mediated reduction of CDC73 has a functional relevance in cell growth and proliferation, we knocked down CDC73 expression in HEK293 cells using miR-155 expressing construct pcDNA3.1(+)-bic and quantitated cell proliferation and cell death (apoptosis) by MTT and CASP3 assays, respectively. As expected, the results demonstrated that the reduced CDC73 level is associated with an increased cell proliferation and decreased apoptosis (Fig. 4*A*). Because KB cells have a high endogenous level of miR-155 (Fig. 1*B*), we knocked it down using antagomir-155. The results showed that the CDC73 levels went up, resulting in decreased cell proliferation and enhanced apoptosis (Fig. 4*B*). Because a given miRNA can target several genes, we assessed the tumorigenic potential of miR-155 by targeting CDC73. The *CDC73* construct (pcDNA3-HA-CDC73) was cotransfected with pcDNA3.1(+)-bic into HEK293 cells, and their proliferation and apoptosis were measured. Interestingly, the CDC73 abrogated the pro-oncogenic effect of miR-155 in HEK293 cells (Fig. 4*C*),

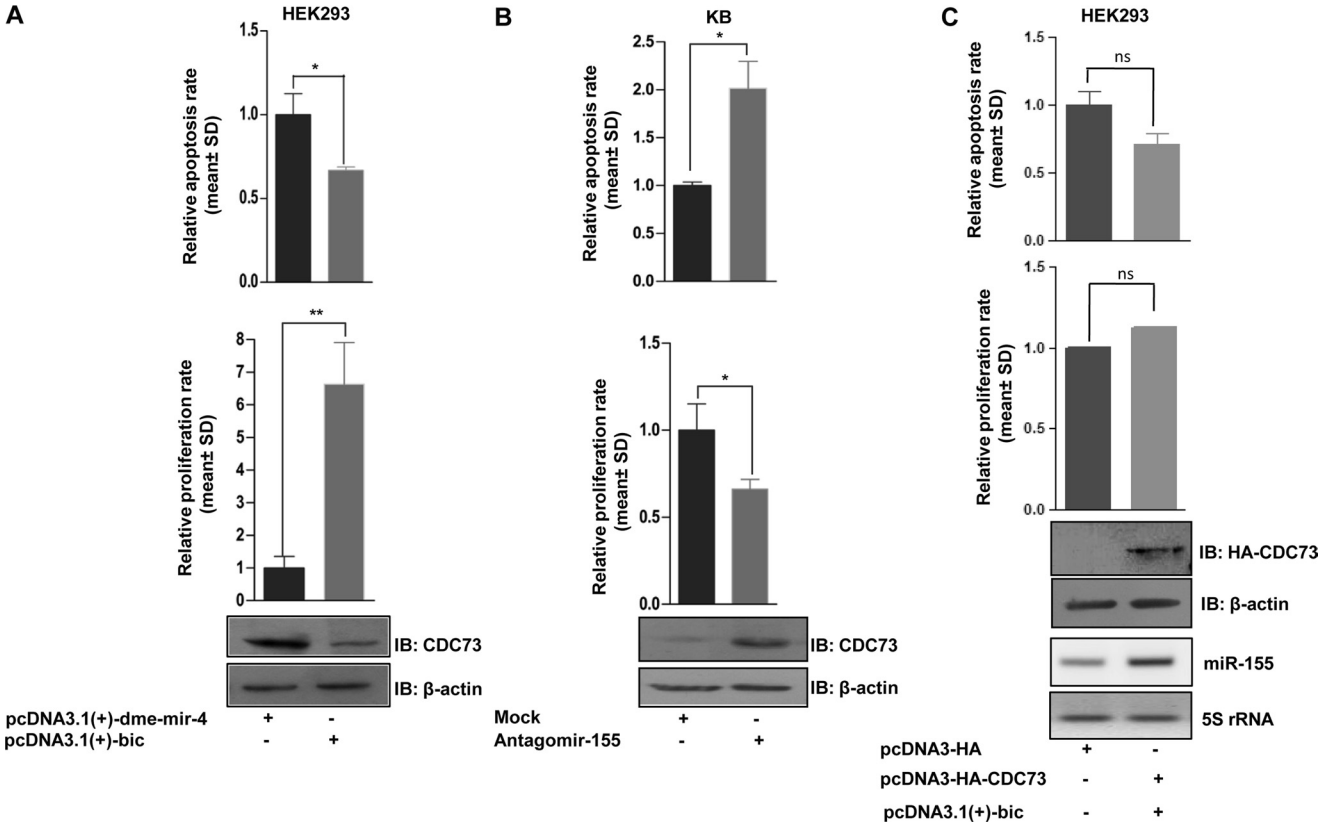

FIGURE 4. **Regulation of cell proliferation and apoptosis by *CDC73* as a target of miR-155.** *A*, overexpression of miR-155 (pcDNA3.1(+)-bic) leads to a significantly reduced CDC73 expression, resulting in increased cell growth and proliferation and decreased apoptosis in HEK293 cells compared with cells transfected with a non-relevant *Drosophila* miRNA pcDNA3.1(+)-dme-mir-4 construct. *IB*, immunoblot. *B*, knockdown of miR-155 by antagomir-155 led to an increased CDC73 expression, resulting in reduced cell growth and proliferation and increased apoptosis in KB cells compared with cells transfected with a non-relevant scrambled oligo (mock). *C*, *CDC73* overexpression abrogated the effect of miR-155 overexpression on proliferation and apoptosis in HEK293 cells. $n = 3$; *ns*, data are statistically non-significant; *, $p < 0.05$; **, $p < 0.01$.

although not completely. These results suggested that miR-155 regulates cell growth and proliferation largely by targeting *CDC73*.

CDC73 Is Down-regulated in OSCC Samples with Up-regulation of miR-155—After validating *CDC73* as a target of miR-155 by bioinformatics and *in vitro* assays, we analyzed the expression of miR-155 by qRT-PCR in OSCC samples. The results showed a significant up-regulation of miR-155 in 16/22 OSCC samples as compared with their matched normal oral tissues (Fig. 5*A*). Furthermore, we also analyzed the expression of CDC73 in 18 of these 22 samples. As expected, a majority of OSCC samples (10/18) having a high expression of miR-155 showed a low level of CDC73 (Fig. 5, *A* and *B*). To exclude the possibility of alternate mechanisms as the cause of CDC73 down-regulation in OSCC, all the 10 OSCC samples were analyzed for LOH at the *CDC73* locus, somatic mutations, and promoter methylation. The results showed that these 10 OSCC samples did not show any mutation, promoter methylation, or LOH (supplemental Table S1), again validating the fact that *CDC73* is a biological target of oncogenic miR-155 and possibly could be the major mechanism for *CDC73* down-regulation in OSCC.

Restoration of CDC73 Expression by miR-155 Inhibition Suppresses Tumor Growth in Vivo—Based on the results of *in vitro* studies, we hypothesized that the abolition of miR-155 and the restoration of tumor suppressor *CDC73* expression in KB cells might have an anti-tumor effect *in vivo*. To address this critical question, we used an *in vivo* pretreated xenograft nude mouse model. Briefly, we transfected the antagomir-155 and scrambled oligos (mock) separately in KB cells. Post 24 h of transfection, these cells were injected separately into nude mice. The mice were observed for the growth of tumors till 23 days. As expected, pretransfection of antagomir-155 into KB cells led to a significant reduction in both tumor volume and weight as compared with mock transfectant (Fig. 6).

DISCUSSION

The 3′-UTR of the human *CDC73* gene is almost 4 kb long, whereas the mean size of 3′-UTRs of human genes is around 800 nucleotides (29). It also contains Alu sequences that have been recently reported as the donors of potential miRNA target sites (30). As mentioned before, a complete loss of CDC73 expression has been reported in a subset of parathyroid carcinomas in the absence of promoter methylation with a single detectable somatic mutation and retention of the wild-type allele (15). These observations suggested that *CDC73* expression could be regulated through its 3′-UTR. In this study we found that miR-155 has a key role in regulating *CDC73* expression. We provide a combination of *in silico, in vitro,* and *in vivo* evidence including a series of miRNA transfection experiments in support of this conclusion.

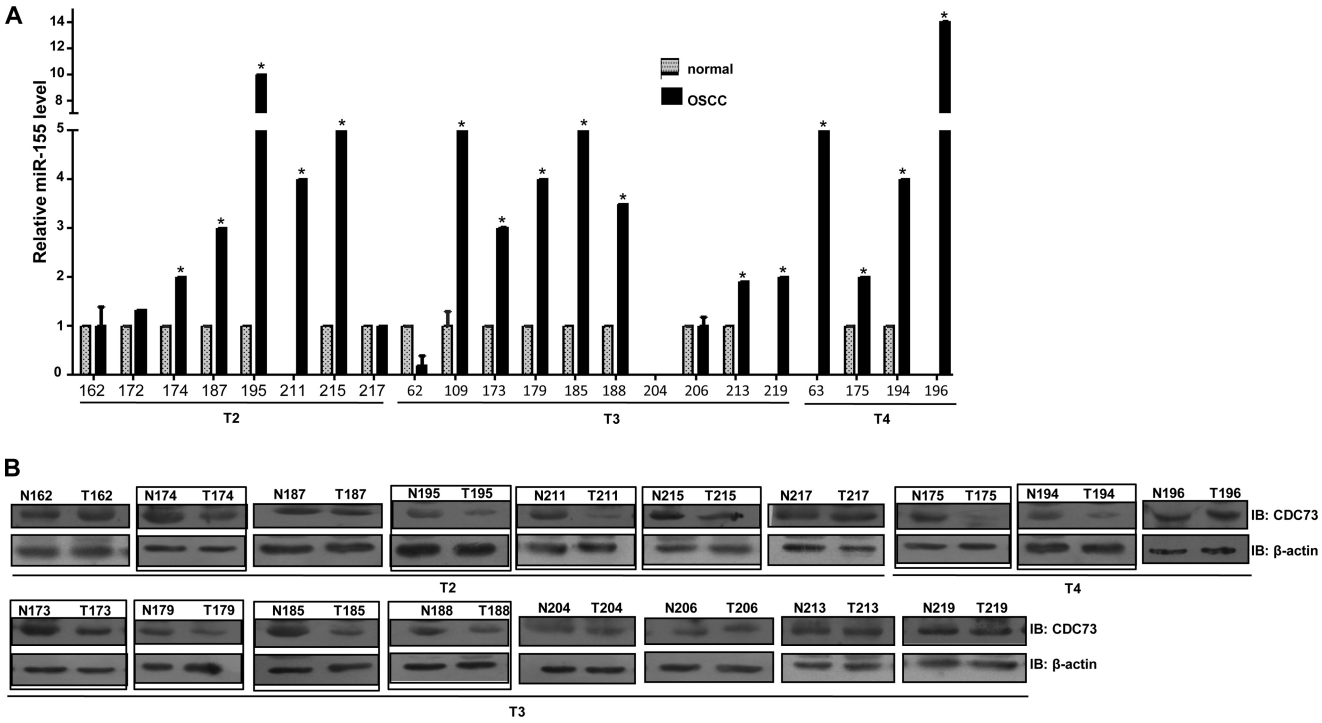

FIGURE 5. **Up-regulation of miR-155 in OSCC samples with reduced expression of CDC73.** *A*, mir-Q RT-PCR was performed to assess the level of miR-155 in matched OSCC and normal oral tissues ($n = 22$). Note a significant up-regulation of miR-155 levels in 16/22 OSCC samples compared with their matching normal samples ($p < 0.05$). No miR-155 expression was detected in normal samples from patients #211, 219, 63, and 196. The relative expression of miR-155 in tumor samples from these patients was calculated relative to the average expression of miR-155 in the rest of the normal samples. Both normal and tumor tissues of patient #204 did not show miR-155 expression upon analysis by mir-Q RT-PCR. *B*, shown is Western blot (*IB*) analysis to assess the expression of CDC73 in 18 matched OSSC and normal oral tissue samples. Note the down-regulation of CDC73 in 10 samples (marked by a *rectangle*) in comparison to their matching normal counterparts; this down-regulation occurs even in the early stages of OSCC development (see tumor samples from patient #174, 195, 211, and 215). Also note that all the 10 OSCC samples showing reduced CDC73 expression have a significant up-regulation of miR-155. The numbers represent different patients. *T2*, *T3*, and *T4* denote stages of the tumors.

Our study focused on miR-155, a microRNA that has been shown to be highly overexpressed in lymphomas of activated-B-cell origin, including Hodgkin's lymphoma (31, 32) and diffuse large B-cell lymphoma (33). Not an exclusive bane of lymphoid cells, miR-155 has also been detected at elevated levels in the bone marrow of some patients suffering with acute myeloid leukemia (34). miR-155 overexpression has additionally been observed in solid tumors of diverse origin (*e.g.* breast, lung, stomach, prostrate, colon, thyroid, pancreatic, and head and neck squamous cell carcinoma) (35–39). All these lines of evidence are consistent with the notion that miR-155 functions as an oncogenic miRNA in human cancers.

As mentioned above, miR-155 is overexpressed in many human cancers. But the mechanisms by which it functions as a putative oncogenic miRNA are largely unknown. Oncogenic miRNAs, which are overexpressed in tumors, function in tumor development mainly via repressing the expression of genes having anti-tumoral activity (40, 41). Of note, miR-155 promotes pancreatic tumor development and mammary gland epithelial cell migration and invasion via targeting the tumor suppressors *TP53INP1* and *RhoA*, respectively (42, 43). In addition, miR-155 induces B-cell malignancies by targeting *Ship* and *C/EBPβ* in a transgenic mouse model (44). Given the scenario that miRNAs usually regulate a large set of targets, there might be more miR-155 targets having anti-tumoral activity. *CDC73*, having anti-tumoral activity, could be one of them.

Our finding of a differential level of miR-155 in various cell lines (Fig. 1*B*) and a subset of paired normal and OSCC samples (Fig. 5*A*) supports that the miR-155-mediated control of *CDC73* is operational in cells that actively produce it. Furthermore, the expression analysis of miR-155 showed that it is highly enriched in a majority of OSCC samples compared with their normal counterparts and had an inverse effect on CDC73 expression, suggesting its key role in the pathogenesis of OSCC by targeting CDC73 (Fig. 5, *A* and *B*). Overexpression of miR-155 down-regulated *CDC73* expression at the protein level in HEK293T cells, but there was no change at the RNA level (Fig. 1*C*). Pertinently, this change at the protein level, but not at the transcript level, has also been reported for other validated targets of miR-155 like *AT1R* (45). Furthermore, the effect of CDC73 differential overexpression was reflected on the proliferation, anchorage-independent growth, and apoptosis of KB cells stably transfected with different *CDC73* constructs (Fig. 3). Overexpression of miR-155 not only led to the knockdown of *CDC73* but also inversed the effect of *CDC73* by promoting proliferation and suppression of apoptosis (Fig. 4*A*). Restoration of CDC73 by knockdown of miR-155 using antagomir-155 was accompanied by decreased cell proliferation, enhanced apoptosis, and reduction of tumor growth in xenograft pretreated model (Figs. 4*B* and 6). Furthermore, the combined overexpression of *CDC73* and miR-155 into HEK293 cells abrogated the oncogenic potential of miR-155 (Fig. 4*C*). Thus, our

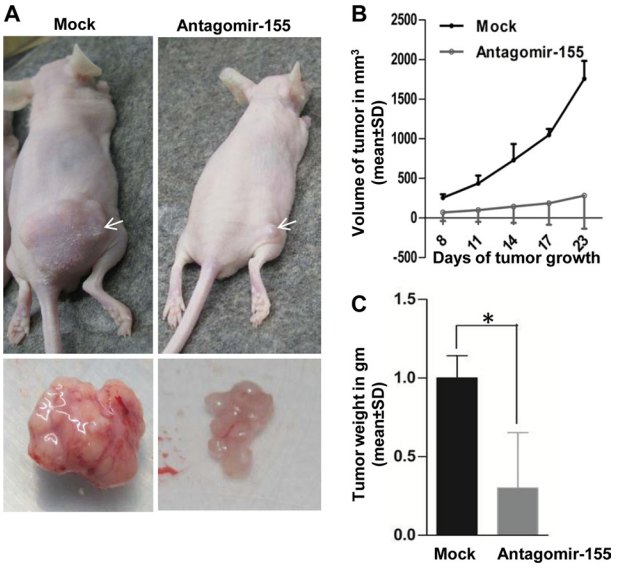

FIGURE 6. **miR-155 inhibition suppresses tumorigenicity *in vivo* in BALB/c nude mice.** *A*, shown is the effect ofantagomir-155 pretreatment to KB cells on tumor formation in a nude mouse xenograft model. Scrambled oligo-transfected (*mock*, *left panel*) and antagomir-155-transfected KB cells (*right panel*) were subcutaneously injected into posterior right flanks of nude mice ($n = 6$). Photographs illustrate representative features of tumor growth on day 23 after injection. *Arrows* mark the xenografts. Excised xenografts are shown *below*. *B*, shown is the effect of the antagomir-155 on tumor volume as compared with mock-treated KB cells during a time course of 23 days. *C*, shown is the effect of the antagomir-155 on tumor weight as compared with mock-treated KB cells. The graph illustrates the weight difference on day 23 after injection. Note that the pretreatment of KB cells with antagomir-155 significantly reduces the tumor volume and weight in nude mice xenografts. *, $p < 0.05$.

findings highlight the key role that *CDC73* plays in orchestration and functional maintenance of oral tissue.

High expression levels of miR-155 have been found to correlate with poor prognoses of lung cancer and pancreatic tumor (38, 46). Our results on therapeutic delivery of antagomir-155 *in vivo* provide a key to therapeutics of malignant OSCC. Being accessible from outside, the use of nucleic acid drugs such as miRNA inhibitors can be easily and directly injected at the tumor site. This kind of treatment could be more promising in the treatment of OSCC compared with its available therapy because a single-gene-based siRNA therapy aimed against a global gene regulator like miR-155 can be highly specific, more effective due to maximum availability of drug at the tumor site, and possibly free of any harmful side effects. Furthermore, to increase the efficiency of this kind of treatment, nucleic acid drugs can be modified to be more lipophilic that improves their intracellular penetration. Although modest compared with pretreatment model, the intratumoral injection of cholesterylated tumor suppressor miRNA mimics has been successful in regression of tumors in the post treatment xenograft model (18). Nonetheless, combined with the ease and simplicity of the drug delivery to a given tumor site in oral cavity, the use of antagomir-155 could have enormous potential to evolve for further drug development.

Taken together, our study validates tumor suppressor *CDC73* as a target of oncogenic miRNA-155 (miR-155). Furthermore, we suggest that the reversal of pro-oncogenic properties of miR-155 due to its inhibitor puts a promise to the use of this inhibitor in cancer therapeutics.

REFERENCES

1. Shattuck, T. M., Välimäki, S., Obara, T., Gaz, R. D., Clark, O.H., Shoback, D., Wierman, M. E., Tojo, K., Robbins, C. M., Carpten, J. D., Farnebo, L. O., Larsson, C., and Arnold, A. (2003) Somatic and germ line mutations of the *HRPT2* gene in sporadic parathyroid carcinoma. *N. Engl. J. Med.* **349,** 1722–1729
2. Aldred, M. J., Talacko, A. A., Savarirayan, R., Murdolo, V., Mills, A. E., Radden, B. G., Alimov, A., Villablanca, A., and Larsson, C. (2006) Dental findings in a family with hyperparathyroidism. Jaw tumour syndrome and a novel *HRPT2* gene mutation. *Oral Surg. Oral Med. Oral Pathol. Oral Radiol. Endod.* **101,** 212–218
3. Pimenta, F. J., Gontijo Silveira, L.F., Tavares, G. C., Silva, A. C., Perdigão, P. F., Castro, W. H., Gomez, M. V., Teh, B. T., De Marco, L., and Gomez, R. S. (2006) HRPT2 gene alterations in ossifying fibroma of the jaws. *Oral. Oncol.* **42,** 735–739
4. Carpten, J. D., Robbins, C. M., Villablanca, A., Forsberg, L., Presciuttini, S., Bailey-Wilson, J., Simonds, W. F., Gillanders, E. M., Kennedy, A. M., Chen, J. D., Agarwal, S. K., Sood, R., Jones, M. P., Moses, T. Y., Haven, C., Petillo, D., Leotlela, P. D., Harding, B., Cameron, D., Pannett, A. A., Höög, A., Heath, H., 3rd, James-Newton, L. A., Robinson, B., Zarbo, R. J., Cavaco, B. M., Wassif, W., Perrier, N. D., Rosen, I. B., Kristoffersson, U., Turnpenny, P. D., Farnebo, L. O., Besser, G. M., Jackson, C. E., Morreau, H., Trent, J. M., Thakker, R. V., Marx, S. J., Teh, B. T., Larsson, C., and Hobbs, M. R. (2002) HRPT2, encoding parafibromin, is mutated in hyperparathyroidism. Jaw tumour syndrome. *Nat. Genet.* **32,** 676–680
5. Bradley, K. J., Cavaco, B. M., Bowl, M. R., Harding, B., Young, A., and Thakker, R. V. (2005) Utilisation of a cryptic non-canonical donor splice site of the gene encoding PARAFIBROMIN is associated with familial isolated primary hyperparathyroidism. *J. Med. Genet.* **42,** e51
6. Wang, P. F., Tan, M. H., Zhang, C., Morreau, H., and Teh, B. T. (2005) HRPT2, a tumour suppressor gene for hyperparathyroidism-jaw tumour syndrome. *Horm. Metab. Res.* **37,** 380–383
7. Krogan, N. J., Dover, J., Wood, A., Schneider, J., Heidt, J., Boateng, M. A., Dean, K., Ryan, O. W., Golshani, A., Johnston, M., Greenblatt, J. F., and Shilatifard, A. (2003) The Paf1 complex is required for histone H3methylation by COMPASS and Dot1p. Linking transcriptional elongation to histone methylation. *Mol. Cell* **11,** 721–729
8. Wood, A., Krogan, N. J., Dover, J., Schneider, J., Heidt, J., Boateng, M. A., Dean, K., Golshani, A., Zhang, Y., Greenblatt, J. F., Johnston, M., and Shilatifard, A. (2003) Bre1, an E3 ubiquitin ligase required for recruitment and substrate selection of Rad6 at a promoter. *Mol. Cell* **11,** 267–274
9. Rozenblatt-Rosen, O., Hughes, C. M., Nannepaga, S. J., Shanmugam, K. S., Copeland, T. D., Guszczynski, T., Resau, J. H., and Meyerson, M. (2005) The parafibromin tumour suppressor protein is part of a human Paf1 complex. *Mol. Cell. Biol.* **25,** 612–620
10. Yart, A., Gstaiger, M., Wirbelauer, C., Pecnik, M., Anastasiou, D., Hess, D., and Krek, W. (2005) The *HRPT2* tumour suppressor gene product parafibromin associates with human PAF1 and RNA polymerase II. *Mol. Cell. Biol.* **25,** 5052–5060
11. Zhang, C., Kong, D., Tan, M. H., Pappas, D. L., Jr., Wang, P. F., Chen, J., Farber, L., Zhang, N., Koo, H. M., Weinreich, M., Williams, B. O., and Teh, B. T. (2006) Parafibromin inhibits cancer cell growth and causes G_1 phase arrest. *Biochem. Biophys. Res. Commun.* **350,** 17–24
12. James, R. G., Biechele, T. L., Conrad, W. H., Camp, N. D., Fass, D. M., Major, M. B., Sommer, K., Yi, X., Roberts, B. S., Cleary, M. A., Arthur, W. T., MacCoss, M., Rawlings, D. J., Haggarty, S. J., and Moon, R. T. (2009) Bruton's tyrosine kinase revealed as a negative regulator of Wnt-β-catenin signaling. *Sci. Signal.* **2,** ra25
13. Cetani, F., Pardi, E., Borsari, S., Viacava, P., Dipollina, G., Cianferotti, L., Ambrogini, E., Gazzerro, E., Colussi, G., Berti, P., Miccoli, P., Pinchera, A., and Marcocci, C. (2004) Genetic analyses of the *HRPT2* gene in primary hyperparathyroidism. Germline and somatic mutations in familial and sporadic parathyroid tumors. *J. Clin. Endocrinol. Metab.* **89,** 5583–5591
14. Hewitt, K. M., Sharma, P. K., Samowitz, W., and Hobbs, M. (2007) Aberrant methylation of the *HRPT2* gene in parathyroid carcinoma. *Ann. Otol. Rhinol. Laryngol.* **116,** 928–933
15. Hahn, M. A., Howell, V. M., Gill, A. J., Clarkson, A., Weaire-Buchanan, G.,

Robinson, B., B., Delbridge, L., Gimm, O., Schmitt, W. D., Teh, B. T., and Marsh, D. J. (2010) *CDC73*/*HRPT2* CpG island hypermethylation and mutation of 5′-untranslated sequence are uncommon mechanisms of silencing parafibromin in parathyroid tumors. *Endocr. Relat. Cancer* **17,** 273–282
16. Mehrotra, R., and Yadav, S. (2006) Oral squamous cell carcinoma. Etiology, pathogenesis, and prognostic value of genomic alterations. *Indian J. Cancer* **43,** 60–66
17. Landis, S. H., Murray, T., Bolden, S., and Wingo, P. A. (1999) Cancer statistics. *CA Cancer J. Clin.* **49,** 8–31
18. Wu, S., Lin, Y., Xu, D., Chen, J., Shu, M., Zhou, Y., Zhu, W., Su, X., Zhou, Y., Qiu, P., and Yan, G. (2012) MiR-135a functions as a selective killer of malignant glioma. *Oncogene* **31,** 3866–3874
19. Bartel, D. P. (2004) MicroRNAs. Genomics, biogenesis, mechanism, and function. *Cell* **116,** 281–297
20. Zhang, W., Dahlberg, J. E., and Tam, W. (2007) MicroRNAs in tumorigenesis. *Am. J. Pathol.* **171,** 728–738
21. Sobin, L. H., and Fleming, I. D. (1997) TNM classification of malignant tumors, fifth edition. Union Internationale Centre le Cancer and the American Joint Committee on Cancer. *Cancer* **80,** 1803–1804
22. Vaz, C., Ahmad, H. M., Sharma, P., Gupta, R., Kumar, L., Kulshreshtha, R., and Bhattacharya, A. (2010) Analysis of microRNA transcriptome by deep sequencing of small RNA libraries of peripheral blood. *BMC Genomics* **11,** 288
23. Kuhn, D. E., Martin, M. M., Feldman, D. S., Terry, A. V. Jr., Nuovo, G. J., and Elton, T. S. (2008) Experimental validation of miRNA targets. *Methods* **44,** 47–54
24. Eis, P. S., Tam, W., Sun, L., Chadburn, A., Li, Z., Gomez, M. F., Lund, E., and Dahlberg, J. E. (2005) Accumulation of miR-155 and BIC RNA in human B cell lymphomas. *Proc. Natl. Acad. Sci. U.S.A.* **102,** 3627–3632
25. Sharbati-Tehrani, S., Kutz-Lohroff, B., Bergbauer, R., Scholven, J., and Einspanier, R. (2008) miR-Q. A novel quantitative RT-PCR approach for the expression profiling of small RNA molecules such as miRNAs in a complex sample. *BMC Mol. Biol.* **9,** 34
26. Livak, K. J., and Schmittgen, T. D. (2001) Analysis of relative gene expression data using real-time quantitative PCR and the $2^{-\Delta\Delta CT}$ method. *Methods* **25,** 402–408
27. Chakraborty, S., Mohiyuddin, S. M., Gopinath, K. S., and Kumar, A. (2008) Involvement of TSC genes and differential expression of other members of the mTOR signaling pathway in oral squamous cell carcinoma. *BMC Cancer* **8,** 163
28. Jiang, L., Dai, Y., Liu, X., Wang, C., Wang, A., Chen, Z., Heidbreder, C. E., Kolokythas, A., and Zhou, X. (2011) Identification and experimental validation of G protein α inhibiting activity polypeptide 2 (GNAI2) as a microRNA-138 target in tongue squamous cell carcinoma. *Hum. Genet.* **129,** 189–197
29. Mignone, F., Gissi, C., Liuni, S., and Pesole, G. (2002) Untranslated regions of mRNAs. *Genome Biology* **3,** S0004
30. Daskalova, E., Baev, V., Rusinov, V., and Minkov, I. (2006) 3′-UTR-located *Alu* e*lements*. Donors of potential miRNA target sites and mediators of network miRNA-based regulatory interactions. *Evol. Bioinform. Online* **2,** 103–120
31. van den Berg, A., Kroesen, B. J., Kooistra, K., de Jong, D., Briggs, J., Blokzijl, T., Jacobs, S., Kluiver, J., Diepstra, A., Maggio, E., and Poppema, S. (2003) High expression of B-cell receptor inducible gene BIC in all subtypes of Hodgkin lymphoma. *Genes Chromosomes Cancer* **37,** 20–28
32. Kluiver, J., Poppema, S., de Jong, D., Blokzijl, T., Harms, G., Jacobs, S., Kroesen, B. J., and van den Berg, A. (2005) BIC and miR-155 are highly expressed in Hodgkin, primary mediastinal and diffuse large B cell lymphomas. *J. Pathol.* **207,** 243–249
33. Costinean, S., Zanesi, N., Pekarsky, Y., Tili, E., Volinia, S., Heerema, N., and Croce, C. M. (2006) Pre-B cell proliferation and lymphoblastic leukemia/high-grade lymphoma in E (mu)-miR155 transgenic mice. *Proc. Natl. Acad. Sci. U.S.A.* **103,** 7024–7029
34. O'Connell, R. M., Rao, D. S., Chaudhuri, A. A., Boldin, M. P., Taganov, K. D., Nicoll, J., Paquette, R. L., and Baltimore, D. (2008) Sustained expression of microRNA-155 in hematopoietic stem cells causes a myeloproliferative disorder. *J. Exp. Med.* **205,** 585–594
35. Iorio, M. V., Ferracin, M., Liu, C. G., Veronese, A., Spizzo, R., Sabbioni, S., Magri, E., Pedriali, M., Fabbri, M., Campiglio, M., Ménard, S., Palazzo, J. P., Rosenberg, A., Musiani, P., Volinia, S., Nenci, I., Calin, G. A., Querzoli, P., Negrini, M., and Croce, C. M. (2005) MicroRNA gene expression deregulation in human breast cancer. *Cancer Res.* **65,** 7065–7070
36. Volinia, S., Calin, G. A., Liu, C. G., Ambs, S., Cimmino, A., Petrocca, F., Visone, R., Iorio, M., Roldo, C., Ferracin, M., Prueitt, R. L., Yanaihara, N., Lanza, G., Scarpa, A., Vecchione, A., Negrini, M., Harris, C. C., and Croce C. M. (2006) A microRNA expression signature of human solid tumors defines cancer gene targets. *Proc. Natl. Acad. Sci. U.S.A.* **103,** 2257–2261
37. Nikiforova, M. N., Tseng, G. C., Steward, D., Diorio, D., and Nikiforov, Y. E. (2008) Micro-RNA expression profiling of thyroid tumors. Biological significance and diagnostic utility. *J. Clin. Endocrinol. Metab.* **93,** 1600–1608
38. Yanaihara, N., Caplen, N., Bowman, E., Seike, M., Kumamoto, K., Yi, M., Stephens, R. M., Okamoto, A., Yokota, J., Tanaka, T., Calin, G. A., Liu, C. G., Croce, C. M., and Harris, C. C. (2006) Unique microRNA molecular profiles in lung cancer diagnosis and prognosis. *Cancer Cell* **9,** 189–198
39. Xiqiang, L., Zugen, C., Jinsheng, Y., James, X., and Xiaofeng, Z. (2009) MicroRNA profiling and head and neck cancer. *Comp. Funct. Genomics*, 11 pp.
40. Esquela-Kerscher, A., and Slack, F. J. (2006) Oncomirs-microRNAs with a role in cancer. *Nat. Rev. Cancer* **6,** 259–269
41. Kent, O. A., and Mendell, J. T. (2006) A small piece in the cancer puzzle. Micro-RNAs as tumor suppressors and oncogenes. *Oncogene* **25,** 6188–6196
42. Gironella, M., Seux, M., Xie, M. J., Cano, C., Tomasini, R., Gommeaux, J., Garcia, S., Nowak, J., Yeung, M. L., Jeang, K. T., Chaix, A., Fazli, L., Motoo, Y., Wang, Q., Rocchi, P., Russo, A., Gleave, M., Dagorn, J. C., Iovanna, J. L., Carrier, A., Pébusque, M. J., and Dusetti, N. J. (2007) Tumor protein 53-induced nuclear protein 1 expression is repressed by miR-155 and its restoration inhibits pancreatic tumor development. *Proc. Natl. Acad. Sci. U.S.A.* **104,** 16170–16175
43. Kong, W., Yang, H., He, L., Zhao, J. J., Coppola, D., Dalton, W. S., and Cheng, J. Q. (2008) MicroRNA-155 is regulated by the transforming growth factor β/Smad pathway and contributes to epithelial cell plasticity by targeting RhoA. *Mol. Cell. Biol.* **28,** 6773–6784
44. Costinean, S., Sandhu, S. K., Pedersen, I. M., Tili, E., Trotta, R., Perrotti, D., Ciarlariello, D., Neviani, P., Harb, J., Kauffman, L. R., Shidham, A., and Croce, C. M. (2009) Src homology 2 domain-containing inositol-5-phosphatase and CCAAT enhancer-binding protein β are targeted by miR-155 in B cells of Eμ-MiR-155 transgenic mice. *Blood* **114,** 1374–1382
45. Zheng, L., Xu, C. C., Chen, W. D., Shen, W. L., Ruan, C. C., Zhu, L. M., Zhu, D. L., and Gao, P. J. (2010) MicroRNA-155 regulates angiotensin II type 1 receptor expression and phenotypic differentiation in vascular adventitial fibroblasts. *Biochem. Biophys. Res. Commun.* **400,** 483–488
46. Greither, T., Grochola, L. F., Udelnow, A., Lautenschläger, C., Würl, P., and Taubert, H. (2010) Elevated expression of microRNAs 155, 203, 210, and 222 in pancreatic tumors associates with poorer survival. *Int. J. Cancer* **126,** 73–80